Annals of Biomedical Engineering, Vol. 34, No. 1, January 2006 *(© 2006)* pp. 15–22
DOI: 10.1007/s10439-005-9001-8

Metal Nanoshells

LEON R. HIRSCH,[1] ANDRE M. GOBIN,[1] AMANDA R. LOWERY,[1] FELICIA TAM,[2] REBEKAH A. DREZEK,[1] NAOMI J. HALAS,[2] and JENNIFER L. WEST [1]

[1]Rice University, Department of Bioengineering, Box 1892, MS 144, Houston, TX 77251-1892, USA and [2]Department of Electrical and Computer Engineering, Box 1892, MS 366, Houston, TX 77251-1892, USA

(Received 19 January 2005; accepted 20 May 2005; published online: 10 March 2006)

Abstract—Metal nanoshells are a new class of nanoparticles with highly tunable optical properties. Metal nanoshells consist of a dielectric core nanoparticle such as silica surrounded by an ultrathin metal shell, often composed of gold for biomedical applications. Depending on the size and composition of each layer of the nanoshell, particles can be designed to either absorb or scatter light over much of the visible and infrared regions of the electromagnetic spectrum, including the near infrared region where penetration of light through tissue is maximal. These particles are also effective substrates for surface-enhanced Raman scattering (SERS) and are easily conjugated to antibodies and other biomolecules. One can envision a myriad of potential applications of such tunable particles. Several potential biomedical applications are under development, including immunoassays, modulated drug delivery, photothermal cancer therapy, and imaging contrast agents.

Keywords—Nanotechnology, immunoassay, controlled release, optical imaging, cancer.

WHAT IS A METAL NANOSHELL?

Medieval alchemists were some of the first to discover the plasmon resonance phenomenon when they successfully reduced gold from a salt solution into its reddish colloidal form. The reddish color arises from the metal colloid's extinction at approximately 520 nm, which results from optical resonances of surface plasmons (or oscillating conducting electrons) in the metal induced by the incident light. Many bulk metals (i.e., Au, Ag, Ni, Pt) demonstrate a plasmon resonance with each metal having a characteristic peak within a defined region of the visible spectrum.[5] Plasmon resonance phenomena of metal colloids have enabled several biomedical applications, but these have been limited by the fact that the plasmon resonances of conventionally available materials fall within the visible range of the spectrum where penetration of light through blood and tissue is low.

Nanoshells are a new class of nanoparticles with tunable plasmon resonance, allowing materials to be specifically designed to match the wavelength required for a particular application, for instance to fall within near infrared (NIR) regions where light penetration through tissue is optimal. Conceived of over 50 years ago[1] but not realized until the 1990's,[3,26,50] a metal nanoshell consists of a spherical dielectric nanoparticle surrounded by an ultrathin, conductive, metallic layer. By varying the composition and dimensions of the layers of the nanoparticles, nanoshells can be designed and fabricated with plasmon resonances from the visible to infrared regions of the spectrum.[27] For a given composition of core and metal shell, the plasmon resonances of the nanoparticle, which determines the particle's optical absorption and scattering, may be tuned by changing the ratio of the nanoparticle's core size to its shell thickness (Fig. 1).

Experimentally, the first metal nanoshell, developed by Zhou *et al*.,[50] consisted of an Au_2S dielectric core surrounded by a gold shell. Depending upon the size of the nanoparticles, it was possible to shift the plasmon resonance to longer wavelengths of light, ranging from the standard gold colloid peak of ~520 out to ~900 nm. Gold-gold sulfide (Au–Au_2S) nanoshells have limits to their size (≤40 nm) and plasmon tunability due their synthesis chemistry. These nanoparticles are grown in a one step process where chloroauric acid ($HAuCl_4$) and sodium sulfide (Na_2S) are mixed. Depending upon the ratios of $HAuCl_4$ and Na_2S added (with an excess of Au), Au–Au_2S nanoshells are grown with different core and shell thicknesses. Due to the kinetics of the core and shell growth[3,4] this synthesis lacks the facility for independent control over nanoparticle core and shell dimensions. Additionally, large amounts of gold colloid are formed as a secondary product of this synthesis scheme, generating an additional absorption peak at ~520 nm.

Oldenburg *et al*. developed a new nanoparticle, a silica-gold core-shell nanoshell, which overcame many of the limitations of the Au–Au_2S particles.[26] To synthesize these particles, a dielectric silica core is grown by the Stöber method,[42] where tetraethylorthosilicate is reduced in ethanol under basic conditions resulting in the nucleation

Address correspondence to Jennifer L. West , Rice University, Department of Bioengineering, Box 1892, MS 144, Houston, TX 77251-1892, USA. Electronic mail: jwest@rice.edu

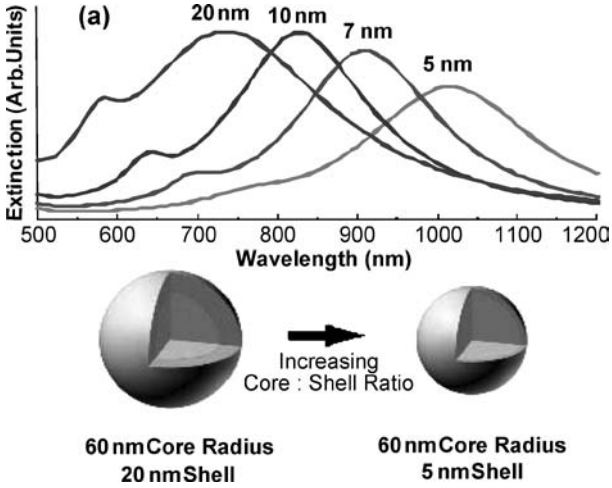

FIGURE 1. Optical tunability is demonstrated for nanoshells with a 60 nm silica core radius and gold shells 5, 7, 10, and 20 nm thick. Observe that the plasmon resonance (extinction) of the particles red shifts with decreasing thickness of the gold shell (or an increasing core:shell ratio). Nanoshells are easily fabricated with resonance in the NIR. Greater tunability can be achieved by also altering the core size, changing the composition of the core and shell, and forming multilayered structures.

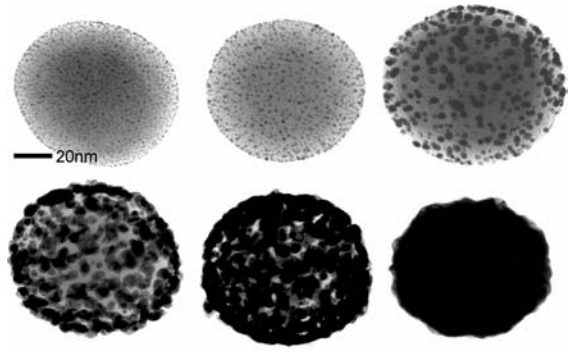

FIGURE 2. Series of TEM images showing gold colloid growth into a complete shell on silica core particle surface. Beginning form the upper left, the gold colloid (dark dots) serve as nucleation sites for additional electroless plating of gold. As additional gold is deposited onto the gold islands, the gold grows until coalescing with neighboring colloid, finally forming a complete metal shell (bottom right).

and growth of highly monodisperse and spherical silica colloid. Particle diameters ranging from 50 to 500 nm can be synthesized by this method. The surfaces of the silica core particles are then functionalized with amine groups by reaction with aminopropyltriethoxysilane (APTES). Small gold colloid (1–2 nm) is then adsorbed onto their aminated surfaces. This disperse surface Au colloid layer serves as nucleation sites for further reduction of gold onto the silica nanoparticle core by reduction of Au in a $HAuCl_4$ solution. As more gold is reduced, the surface coating grows and coalesces into a complete gold shell (Fig. 2). The amount of $HAuCl_4$ added determines the final thickness of the gold shell, which can typically range between 5 and 30 nm. By changing the ratio of the core diameter to shell thickness, the plasmon resonance peak may be placed anywhere within the visible to mid-infrared region of light. More recently, this geometry has been extended into multilayered, concentric nanoshells, producing more complex hybridized resonances whose spectral profiles span the infrared spectrum to thermal wavelengths.[31]

Additionally, metal nanoshells have demonstrated strong surface-enhanced Raman scattering (SERS)—at least 10^{10} enhancements are possible.[18,19,26] Metal films and nanoparticles have been investigated by many groups as substrates for SERS. The tremendous enhancement in Raman scattering for molecules close to such metal surfaces is believed to be due to the local enhanced electromagnetic field at the surface due to the excitation of surface plasmons.[24] Thus, optimal SERS is observed at the plasmon resonance of the substrate material; the tunability of the plasmon resonance of nanoshells is exciting as it may enable one to design a substrate to match the wavelength desired for a given application and to work in the NIR to potentially enable *in vivo* applications of SERS. A NIR SERS nanosensor may be possible for assays performed in whole blood, intracellular spectroscopy, or *in vivo* diagnostics.

Gold nanoshells are particularly attractive for use in biological applications due to the fact that their outer shell is composed of reduced gold. This noble metal is resistant to corrosion, demonstrates low toxicity, and is a popular material for medical applications such as dental prosthetics, which utilize its inert chemical properties and conformational flexibility.[6,9,29] Biomedical applications also use gold in electrodes for amperometric detection of analytes (i.e., O_2, H_2O_2, urea, glucose) in long term sensing applications.[14,21,34] Additionally, gold facilitates easy conjugation of proteins onto its surface. Proteins spontaneously chemisorb to gold surfaces when incubated with the metal at or slightly basic to their isoelectric point. This technique is commonly used for immunogold labeling techniques.[15] However, most current methods prefer a more irreversible, if not covalent, method of molecule immobilization onto gold surfaces. Proteins and other thiol/disulfide-possessing molecules are capable of spontaneously self-assembling into dense networks on gold surfaces. This strong dative interaction between the sulfur and gold is reversible, but strongly favors binding in the forward direction with a bond enthalpy of 126–146 kJ/mol—a strength approaching that of other covalent bonds.[25] Proteins and other synthetic molecules are easily functionalized with these sulfhydryl moieties to create a robust, simple method of tailoring the gold nanoshell surface chemistry, and concomitantly, its bioreactivty/inertness for biosensing or therapeutic applications. Using this type of chemistry, metal nanoshells can be chemically modified with either hydrophobic or hydrophilic species. This provides the advantage of using nanoshells in solution-based systems

without compromising solubility or colloidal stability in either organic or aqueous environments. For *in vivo* applications, nanoshells can be immoblized within "stealthing" polymers or microencapsulated to provide steric stabilization and reduce the risk of opsonization.[12,13]

BIOMEDICAL APPLICATIONS OF METAL NANOSHELLS

Optical methods for diagnosis and treatment in medicine and biology are attractive due to their potential for non-invasive and minimally-invasive applications. NIR light between 700–1100 nm is particularly interesting due to the absence of significant absorption from either biological chromophores or water within this region, permitting deep optical penetration into biological samples such as tissue or whole blood.[48] Numerous diagnostic systems employing NIR optical probes are under investigation. Tomographic techniques, such as optical coherence tomography (OCT), use backscattered light to reconstruct high-resolution images ($\leq$10 μm) of tissue morphology.[17] While OCT has been used most extensively in ophthalmology, it has also examined features such as intimal thickening in human aortae.[7] On a larger scale, tomographic reconstructions of whole brain specimens have been made with NIR light. Although this technique does not approach the spatial resolution of conventional methods (i.e., MRI, CT), it does contain spectral information as well; NIR spectroscopy in conjunction with tomography may provide both space- and time-resolved information about cerebral oxygenation, which is of particular interest in neonates.[16] Some other NIR applications worth mentioning are confocal imaging, iridotomy, and photothermal coagulation—all of which take advantage of tissue's increased transparency within this region.[33,44] As discussed above, metal nanoshells can be easily tuned to have strong scattering or absorption properties in the NIR, enabling many new biomedical applications in this interesting spectral region.

Nanoshells for Immunoassays

Immunoassays utilize antibody-antigen interactions to detect a specific antigen within a complex mixture. The Sandwich-Type Enzyme Linked Immunosorbant Assay (ELISA) is the most widely used immunoassay. Although ELISAs are very effective at detecting small amounts of analyte, they suffer a few limitations. These systems rely upon either fluorescence or a colorimetric change in solution to determine antigen concentrations, making it necessary to use purified, cell-free specimens and perform multiple rinsing steps in order to minimize optical interference and obtain a pure signal. For the analysis of a blood specimen, these additional purification steps may lengthen the time necessary to complete an assay (4–24 h). In addition, these assays are performed on a solid, macroscopic substrate, limiting the application to *in vitro* use only. The ELISA's dependence upon enzymatic activity for detection is another problem, due to its dependence upon temperature, denaturation, pH, and other factors. To overcome these issues, a new immunoassay technique has been developed utilizing antibody conjugated, NIR resonant nanoshells. This assay can be performed in whole blood and provides results within several minutes with sensitivity similar to an ELISA.[12,13]

The underlying mechanism behind the nanoshell-based immunoassay is similar to that of conventional latex agglutination (LA) and sol particle immunoassays (Singer and Plotz, 1956, Leuvering *et al*., 1980). When antibody conjugated particles are exposed to a multivalent analyte, multiple particles will bind to the analyte, forming particle dimers and higher order assemblies of particles. Unfortunately, LA and sol particle assays are difficult to perform in whole blood due to blood's high turbidity and strong visible extinction. The aggregation of nanoshells gives rise to additional optical resonances at longer wavelengths for the aggregate structure since the plasmon resonant spectral response of nanoparticle masses differs significantly from that of isolated, dispersed plasmon resonant nanoparticles.[32] Nanoshell dimers and larger aggregates produce a significantly red-shifted plasmon resonance. The red-shifted plasmon from aggregation is simultaneously accompanied by a decrease in the amplitude of the single nanoshell plasmon resonance in the overall spectral response.[32] This appears in the optical signal as a net shift in the nanoshell resonance to longer wavelengths in the NIR extinction spectrum. This provides a straightforward method for detecting nanoshell-bioconjugate aggregation via monitoring of the decrease in extinction at the original nanoshell plasmon resonance peak, as shown in Fig. 3.[12,13]

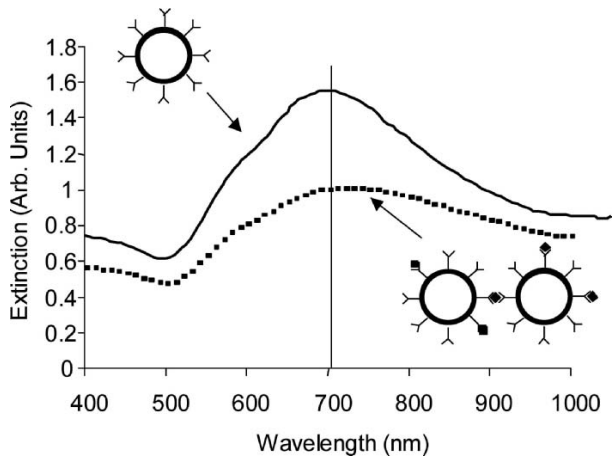

FIGURE 3. The principle of the nanoshell immunoassay. Nanoshells conjugated with antibody specific for a particular analyte are well dispersed in an analyte free environment (–), and possess a spectrum with a resonance in the near infrared. In the presence of analyte, however, antibody-antigen interactions cause nanoshell agglutination, a phenomenon that is easily detected by a reduction in the nanoshell suspension's original peak resonance (–).

The performance of the nanoshell-based immunoassay has been evaluated in saline, serum, and blood samples for a variety of analytes.[12,13] For these assays, antibodies are conjugated to nanoshells via a polyethylene glycol (PEG) linker that is derivatized with thiol groups. Quantitative analyte detection could be achieved over the concentration range of 0.4–400 ng/ml, with completion of the assay in 10 min. The availability of this type of rapid, *in situ*, whole blood assay with the capacity to detect a variety of analytes would greatly benefit point-of-care or public health applications where there is a strong demand for rapid screening of blood-borne species such as bacteria, viruses, or proteins.

Optically-Responsive Nanoshell-Hydrogel Composites

Over the past several decades, the field of controlled drug delivery has faced two major challenges; sustained zero-order release of a therapeutic agent and pulsatile delivery of a therapeutic agent. The first goal has been largely addressed by a variety of delivery systems, including osmotically driven pumps and biodegradable matrices (reviewed in).[40] The second goal, controlled modulation of drug delivery, has proved more difficult. Thermally responsive hydrogels and membranes have been extensively evaluated as platforms for the pulsatile delivery of drugs. One of the characteristics of temperature-responsive hydrogels is the presence of a lower critical solution temperature (LCST), a temperature at which the hydrogel material will undergo a dramatic phase change. The driving force for this phase change is based on the interactions between the polymer and the surrounding water.[35,43] Below the LCST, the most thermodynamically stable configuration is for the water molecules to remain clustered around the polymer chains. Above the LCST, the polymer chains collapse upon each other and minimize interaction with water. Due to this phase change, a macroscopic hydrogel will undergo a drastic change in dimensions, collapsing as the temperature exceeds the LCST, with expulsion of water (and dissolved drug) from the matrix.

N-isopropylacrylamide (NIPAAm) is a commonly used thermoresponsive polymer, and copolymers of NIPAAm and acrylamide form hydrogel materials with LCSTs ranging from 32–60°C, depending on the composition of the copolymer.[30] Pulsatile delivery of a variety of drugs has been demonstrated from NIPAAm-co-acrylamide hydrogels by subjecting the materials to changes in temperature.[30,49] While very nice results have been achieved with this system, the practical implementation of the system has been difficult due to issues with inducing temperature changes in implanted materials. In order to develop NIR responsive materials that might be more easily manipulated implants for modulated drug delivery, composite hydrogels formed from NIPAAm-co-acrylamide and NIR-absorbing nanoshells have been developed.[39] The composites were fabricated by mixing nanoshells into the monomer mixture. After polymerization, the nanoshells were physically entrapped in the hydrogel matrix. As shown in Fig. 4, the composite hydrogels undergo a pronounced collapse in response to NIR light; the nanoshells absorb the light, generating heat within the composite to exceed the LCST of the copolymer, thus inducing the phase change.[37]

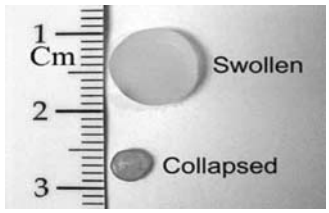

FIGURE 4. Nanoshells entrapped within the NIPAAm-co-acrylamide hydrogels absorb near infrared light to drive the phase change of the thermally responsive polymer. Exceeding the LCST caused collapse of the hydrogel material, due to expulsion of water and collapse of the polymer chains.

The collapse of the hydrogel material is completely reversible. When the temperature falls below the LCST, the polymer chains extend and interact with water, causing the material to swell. The reversible nature of this phenomenon allows one to partially collapse the material, re-swell it, cycling above and below the LCST repeatedly. If a drug has been incorporated into the hydrogel matrix, each time the hydrogel collapses, a burst of drug will be expelled from the material, as demonstrated in Fig. 5.[39] Because of the deep penetration of NIR light through tissue, the composite hydrogels may be implanted subcutaneously, with the phase change behavior easily manipulated by externally applied NIR light.

Recently, these optically responsive composites have been utilized as valves within a microfluidics device.[40] In this case, it is desirable to have independent optical

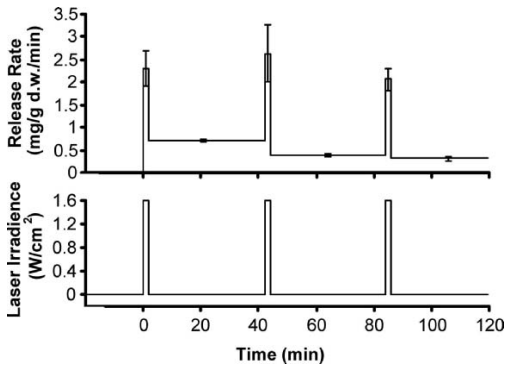

FIGURE 5. Pulsatile release of protein (top panel) from nanoshell composite NIPAAm-co-AAm hydrogels was achieved through pulsatile near infrared irradiation (bottom panel).

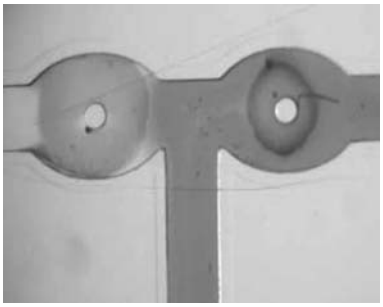

FIGURE 6. Nanoparticle-containing NIPAAm-co-AAm hydrogels were photopolymerized within microfluidics devices to form optically-controlled valves. By changing the optical absorption of the nanoshells within a particular valve, one can determine what wavelengths of light will cause valve opening. In this case, two valves were formed at a T-junction, one that responded to green light while the other responded to NIR light. Independent control of the two valves was obtained. Blue dextran was used to visualize flow patterns.

control over multiple valve structures within a single device, allowing one to control complex flow patterns through a device simply by changing the wavelength of light used for illumination. In such an application, the broad tunability of nanoshells is advantageous. In a preliminary study, independent control over two separate valves at a T-junction has been demonstrated, one opening in response to 532 nm illumination while the other opened upon exposure to light at 832 nm (Fig. 6).[40]

Photothermal Ablation

As discussed above, nanoshells can be designed to strongly absorb NIR light and thus generate localized heating, potentially enabling nanoshell-mediated thermal ablation therapies for applications such as cancer treatment. Thermal ablation therapies can provide a minimally invasive alternative to surgical excision of tumors and are particularly attractive for situations where surgery is not possible. Thermal delivery methods under investigation for local tissue ablation include lasers,[2,45] microwave and radio frequency energy,[8,36] magnetic thermal ablation,[11] and focused ultrasound.[20] The goal of thermal ablation is to conform a lethal dose of heat to a prescribed tissue volume with as little damage to intervening and surrounding normal tissue as possible, which has been difficult with the majority of techniques currently under investigation. Due to the lack of absorption of NIR light by tissue components, use of this type of light source, with nanoshells localized within the tumor site, should minimize collateral tissue damage. *In vitro* studies with nanoshells bound to breast carcinoma cells have demonstrated effective destruction of the cancerous cells upon exposure to near infrared light,[12,13] with cell damage limited to the laser treatment spot (Fig. 7).

The efficacy of nanoshell-mediated photothermal ablation has also been assessed in several *in vivo* studies. Initial studies involved directly injecting nanoshell suspensions into tumor sites and utilizing MRI thermal imaging to monitor temperature profiles during NIR-induced heating.[12,13] These studies demonstrated rapid heating of nanoshell-laden tissues upon exposure to the near infrared light. Evaluation of the gross pathology and histology demonstrated marked tissue damage at the treatment sites, with little or no damage to surrounding tissue. This initial work also provided information about the relationships between nanoshell dosages, light intensity, and duration of illumination with the ultimate thermal profile and resultant tissue damage. However, for the majority of applications, direct injection into the tumor site may not be feasible.

An alternative approach is to inject nanoshells intravenously, allowing them to circulate and accumulate at the tumor site before NIR treatment. The size of nanoshells is critical to the success of this type of approach. Substantial prior research has investigated the delivery of macromolecules and small particles through the tumor vasculature. These efforts have demonstrated that particles in the 60–400 nm size range will extravasate and accumulate in many tumor types via a passive mechanism referred to as the "enhanced permeability and retention" (EPR) effect.[23] This effect has been attributed to the highly proliferative vasculature within neoplastic tumors. During rapid angiogenesis, defects in the vascular architecture are often present, resulting in leaky vessels. Nanoshells fall within the range applicable for the EPR effect, and thus should accumulate in most tumor types following intravenous injection. The efficacy of photothermal ablation following systemic delivery of nanoshells has been evaluated in a mouse model.[28] Complete regression of tumors was observed within 10 days following treatment with nanoshells and near infrared light, with no tumor re-growth over at least 60 days. Survival times for mice with the nanoshell treatment in this study were significantly improved compared to untreated mice or those receiving laser treatment alone. Additionally, it is possible to conjugate nanoshells to antibodies to oncoproteins or endothelial markers, which may improve the accumulation of nanoshells in the tumor tissue and further localize nanoshells to targeted cells at the treatment site.

Nanoshell Contrast Agents in Imaging

The drug delivery and thermal ablation applications described in the preceding sections used nanoshells designed to strongly absorb light in the NIR spectral region. By fabricating nanoshells designed to preferentially scatter rather than absorb light, nanoshells can serve as strong optical contrast agents for a variety of biomedical optical imaging applications. Photonics-based imaging technologies offer

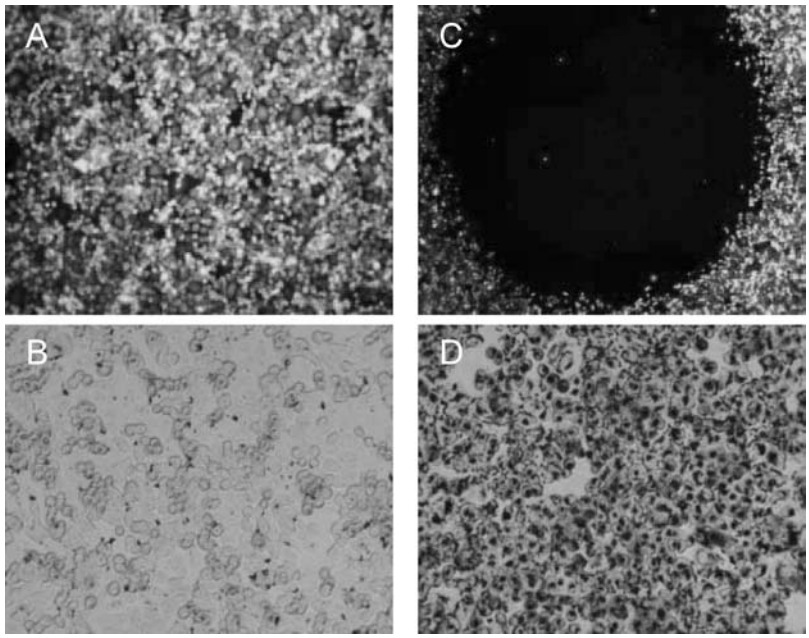

FIGURE 7. HER2-positive breast carcinoma cells were treated with nanoshells conjugated with either a control anti-IgG (panels A and B) or anti-HER2 (panels C and D). Upon NIR laser treatment, cells exposed to anti-HER2 nanoshells were effectively destroyed, as demonstrated by the circular region corresponding to the laser spot that lacks staining with a fluorescent viability marker (C), while the nanoshells bound to the control antibody did not produce this effect. Silver staining was then performed to visualize nanoshell binding to cells. Nanoshells only bound to the breast carcinoma cells when conjugated to the anti-HER2 antibody (control = B, anti-HER2 = D).

the potential for non-invasive, high-resolution *in vivo* imaging. However, the clinical utility of optical imaging strategies has been significantly constrained both by the limited variety of endogenous chromophores present in tissue and by relatively low levels of optical contrast between normal and diseased tissue. Furthermore, in the case of cancer, where early detection is critical to reducing morbidity and mortality, it is often desirable to image specific molecular biomarkers which are present long before pathologic changes occur at the anatomic level. Imaging biomarkers of interest requires development of targetable optical contrast agents. A recent demonstration of scattering-based molecular imaging used gold colloid conjugated to antibodies to the epidermal growth factor receptor (EGFR) as an optical contrast agent for imaging early cervical precancers.[41] While gold colloid bioconjugates are valuable as contrast agents for detecting superficial epithelial cancers with visible light, a primary challenge in optical contrast agent development has been the need for optical contrast agents at the multiple laser wavelengths within in the NIR spectral region commonly used in optical imaging applications. The facile tunability of nanoshells facilitates their use as NIR contrast agents. In addition, nanoshells offer other advantages relative to conventional imaging agents including more favorable optical scattering properties, enhanced biocompatibility, and reduced susceptibility to chemical/thermal denaturation. Furthermore, as described above, nanoshells are readily conjugated to antibodies or other targeting moieties of interest, enabling molecular specific imaging.

Initial *in vitro* studies were conducted to demonstrate the potential of nanoshell bioconjugates for molecular imaging applications. These experiments used nanoshell designed to strongly scatter light throughout the NIR "optical window" of 700–1200 nm. To enable molecular targeting, antibodies were conjugated onto nanoshell surfaces using a PEG linker. Cells incubated with scattering nanoshell bioconjugates were viewed under darkfield microscopy, a form of microscopy sensitive only to scattered light. Significantly increased optical contrast due to expression of HER2, a clinically relevant cancer biomarker, was observed in HER2-positive breast carcinoma cells targeted with HER2-labeled nanoshells compared to the contrast observed in cells targeted by either nanoshells non-specifically labeled with IgG or control cells which were not exposed to nanoshell conjugates (Fig. 8). Recently, it has also been demonstrated that nanoshells designed to have both scattering and absorption components to their extinction can be used for integrated imaging and therapy.[22]

Nanoshells have also been utilized as contrast agents in a very different type of imaging modality—photoacoustic tomography.[46] Photoacoustic tomography (PAT) is a hybrid imaging modality that uses light to rapidly heat elements

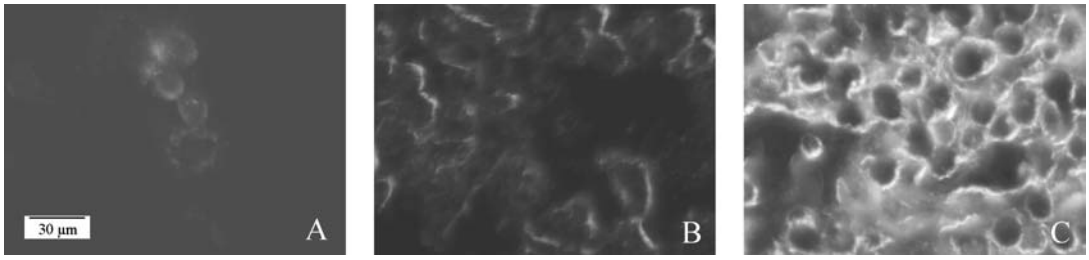

FIGURE 8. Dark field images of HER2-positive breast carcinoma cells A: untreated, B: treated with non-specific anti-IgG conjugated nanoshells or C: treated with anti-HER2-conjugated nanoshells. The nanoshells were designed to be strongly scattering, thus generating bright images of targeted cells observed via dark field microscopy. Length bar = 30 μm.

within tissue; the resultant thermoelastic expansion generates photoacoustic waves that are then detected with an ultrasonic transducer. The use of NIR-absorbing agents, such as metal nanoshells, should generate greater contrast in images due to the more substantial differences in optical absorption and thus in generation of photoacoustic waves than is possible based on endogenous tissue chromophores. In an *in vivo* brain imaging study, PEG-coated, NIR-absorbing gold nanoshells were injected intravenously, then PAT was used to image the cerebral vasculature.[46] Nanoshell injection increased optical absorption in the brain tissue by more than 60%. Moreover, due to the long circulation time of PEG-coated nanoshells, images could be taken for many hours without decreased contrast.[46]

REFERENCES

1. Aden, A. L., and M. Kerker. *J. Appl. Phys.* 22:1242–1246, 1951.
2. Amin, Z., W. Thurrell, G. M. Spencer, S. A. Harries, W. E. Grant, S. G. Bown, W. R. Lees. *Invest. Radiol.* 28:1148–1154, 1993.
3. Averitt, R. D., D. Sarkar, and N. J. Halas. *Phys. Rev. Lett.* 78:4217–4220, 1997.
4. Averitt, R. D., S. L. Westcott, and N. J. Halas. *J. Opt. Soc. Am. B* 16:1824–1832, 1999.
5. Bohren, C. F., and D. R. Huffman. In *Absorption and Scattering of Light by Small Particles*, Wiley-Interscience, New York, pp. 379, 1983.
6. Eichner, K. *Int. Dent. J.* 33:1–10, 1983.
7. Fujimoto, J. G., M. E. Brezinski, B. J. Tearney, S. A. Boppart, B. Bouma, M. R. Hee, J. F. Southern, and E. A. Swanson. *Nat. Med.* 1:970–972, 1995.
8. Gazelle, G. S., S. N. Goldberg, L. Solbiati, and T. Livraghi. *Radiology* 217:633–646, 2000.
9. Hagman, H. *Dent. Lab. Rev.* 54:28–30, 1979.
10. Hilger, I., R. Hiergeist, R. Hergt, K. Winnefeld, H. Schubert, and W. A. Kaiser. *Invest. Radiol.* 37:580–586, 2002.
11. Hirsch, L. R., J. B. Jackson, A. Lee, N. J. Halas, and J. L. West. *Analyt. Chem.* 75:2377–2381, 2003.
12. Hirsch, L. R., R. J. Stafford, J. A. Bankson, S. R. Sershen, B. Rivera, R. E. Price, J. D. Hazle, N. J. Halas, and J. L. West. *Proc. Natl. Acad. Sci. USA* 100:13549–13554, 2003.
13. Holstrum, N., P. Nilsson, J. Carlsten, and S. Bowland. *Biosensors and Bioelectronics* 13:1287–1295, 1998.
14. Horisberger, M., and J. Rosset. *J. Histochem. Cytochem.* 25:295–305, 1977.
15. Houten, J. V., D. Benaron, S. Spilman, and D. K. Stevenson. *Ped. Res.* 39:470–476, 1996.
16. Huang, D., E. A. Swanson, C. P. Lin, J. S. Schuman, W. G. Stinson, W. Chang, M. R. Hee, T. Flotte, K. Gregory, C. A. Puliafito, and J. G. Fujimoto. *Science* 254:1178–1181, 1991.
17. Jackson, J. B., S. L. Westcott, L. R. Hirsch, J. L. West, and N. J. Halas. *Appl. Phys. Lett.* 82:257–259, 2003.
18. Jackson, J. B., and N. J. Halas. *Proc. Natl. Acad. Sci. USA* 101:17930–17935, 2004.
19. Jolesz, F. A., and K. Hynynen. *Cancer J.* S1:100–112, 2002.
20. Leuvering J. H., Thal P. J., van der Waart M., Schuurs A. H. *J. Immunoassay*, 1:77–91, 1980.
21. Lindholm-Sethson, B., J. C. Gonzalez, and G. Puu. *Langmuir* 14:6705–6708, 1998.
22. Loo, C., A. Lowery, N. Halas, J. West, and R. Drezek. *NanoLett.* 5:709–711, 2005.
23. Maeda, H., T. Sawa, and T. Konno. *J. Control. Rel.* 74:46–61, 2001.
24. Maher, R. C., L. F. Cohen, P. Etchegoin, H. J. N. Hartigan, R. J. C. Brown, and M. J. T. Milton. *J. Chem. Phys.* 120:11746–11753, 2004.
25. Nuzzo, R. G., F. A. Fusco, and D. L. Allara. *J. Am. Chem. Soc.* 109:2358–2368, 1987.
26. Oldenburg, S. J., R. D. Averitt, S. L. Westcott, and N. J. Halas. *Chem. Phys. Lett.* 28:243–247, 1998.
27. Oldenburg, S. J., S. L. Westcott, R. D. Averitt, and N. J. Halas. *J. Chem. Phys.* 111:4729–4735, 1999.
28. O'Neal, D. P., L. R. Hirsch, N. J. Halas, J. D. Payne, and J. L. West. *Cancer Lett.*, In Press, 2004.
29. Pourbaix, M. *Biomaterials* 5:122–134, 1984.
30. Priest, J. H., S. L. Murray, R. J. Nelson, and A. S. Hoffman. *Revers. Polym. Gels Relat. Syst.* 350:255–264, 1987.
31. Prodan, E., C. Radloff, N. Halas, and P. Nordlander, *Science* 302:419–422, 2003.
32. Quinten, M. *Appl. Phys. B* 73:317–326, 2001.
33. Rajadhyaksha, M., S. González, J. M. Zavislan, R. R. Anderson, and R. H. Webb. *J. Invest. Dermatol.* 113:203–303, 1999.
34. Ruan, C., R. Yang, X. Chen, and J. Deng. *J. Electroanal. Chem.* 455:121–125, 1998.
35. Sasaki, S., H. Kawasaki, and H. Maeda. *Macromolecules* 30:1847–1848, 1997.
36. Seki, T., M. Wakabayashi, T. Nakagawa, M. Imamura, T. Tamai, A. Nishimura, N. Yamashiki, A. Okamura, and K. Inoue. *Cancer* 85:1694–1702, 1999.
37. Singer J. M. and Plotz, C. M. *Am. J. Med.* 21:888–892, 1956.
38. Sershen, S., and J. West. *Adv. Drug Del. Rev.* 54:1225–1235, 2002.

[39.] Sershen, S. R., J. L. Westcott, J. L. West, and N. J. Halas. *Appl. Phys. B* 73:379–381, 2001.
[40.] Sershen S.R., Mensing G. A., Ng M., Halas N.J., Beebe D. J. West J. L. *Adv. Mat*., 17:1366–1368, 2005.
[41.] Sershen, S. R., S. L. Westcott, N. J. Halas, and J. L. West. *J. Biomed. Mater. Res*. 51:293–298, 2000.
[42.] Sershen, S. R., S. L. Westcott, N. J. Halas, and J. L. West. *Appl. Phys. Lett*. 80:4609–4611, 2002.
[43.] Sokolov, K., M. Follen, I. Pavolva, A. Malpica, R. Lotan, and R. Richards-Kortum. *Cancer Res*. 63:1999–2004, 2003.
[44.] Stober, W., and A. Fink. *J. Colloid. Interf. Sci*. 26:62–69, 1968.
[45.] Tanaka, N., S. Matsukawa, H. Kuroso, and I. Ando. *Polymer* 39:4703–4706, 1998.
[46.] Vogel, A. *Phys. Med. Biol*. 42:895–912, 1997.
[47.] Vogl, T. J., M. G. Mack, R. Straub, K. Engelmann, S. Zangos, and K. Eichler. *Radiologe* 39:764–771, 1999.
[48.] Wang, Y., X. Xie, X. Wang, G. Ku, K. L. Gill, D. P. O'Neal, G. Stoica, and L. V. Wang. *NanoLett*. 4:1689–1692, 2004.
[49.] Weissleder, R. *Nat. Biotech*. 19:316–317, 2001.
[50.] Welch, A., and M. van Gemert (Eds). *Optical-Thermal Response of Laser-Irradiated Tissue*, Plenum Press, New York, 1995.
[51.] Yoshida, R., K. Sakai, T. Okano, and Y. Sakurai. *J. Biomat. Sci. Polym. Ed*. 6:585–598, 1994.
[52.] Zhou, H. S., I. Honma, and H. Komiyama. *Phys. Rev. B* 50:12052–12056, 1994.